Advances in Water Resources 98 (2016) 16–31

Contents lists available at ScienceDirect

Advances in Water Resources

journal homepage: www.elsevier.com/locate/advwatres

Integrating a reservoir regulation scheme into a spatially distributed hydrological model☆

Gang Zhao[a], Huilin Gao[a,*], Bibi S. Naz[b], Shih-Chieh Kao[b], Nathalie Voisin[c]

[a] Zachry Department of Civil Engineering, Texas A&M University, College Station, TX 77843, United States
[b] Environmental Sciences Division and Climate Change Science Institute, Oak Ridge National Laboratory, Oak Ridge, TN 37831, United States
[c] Hydrology Group, Pacific Northwest National Laboratory, Richland, WA 99352, United States

ARTICLE INFO

Article history:
Received 27 January 2016
Revised 29 August 2016
Accepted 13 October 2016
Available online 14 October 2016

Keywords:
Reservoir
DHSVM
Water resources
Operation rules

ABSTRACT

During the past several decades, numerous reservoirs have been built across the world for a variety of purposes such as flood control, irrigation, municipal/industrial water supplies, and hydropower generation. Consequently, the timing and magnitude of natural streamflow have been altered significantly by reservoir operations. In addition, the hydrological cycle is also modified by land-use/land-cover change and by climate change. To understand the fine-scale feedback between hydrological processes and water management decisions, a distributed hydrological model embedded with a reservoir component is desired. In this study, a multi-purpose reservoir module with predefined complex operational rules was integrated into the Distributed Hydrology Soil Vegetation Model (DHSVM). Conditional operating rules, which are designed to reduce flood risk and enhance water supply reliability, were adopted in this module. The performance of the integrated model was tested over the upper Brazos River Basin in Texas, where two U.S. Army Corps of Engineers managed reservoirs, Lake Whitney and Aquilla Lake, are located. The integrated model was calibrated and validated using observed reservoir inflow, outflow, and storage data. The error statistics were summarized for both reservoirs on a daily, weekly, and monthly basis. Using the weekly reservoir storage for Lake Whitney as an example, the coefficient of determination (R^2) was 0.85 and the Nash-Sutcliff Efficiency (NSE) was 0.75. These results suggest that this reservoir module holds promise for use in sub-monthly hydrological simulations. With the new reservoir component, the DHSVM provides a platform to support adaptive water resources management under the impacts of evolving anthropogenic activities and substantial environmental changes.

1. Introduction

To maximize the benefits from limited freshwater resources, and to mitigate flood risks, numerous reservoirs have been constructed during the past several decades throughout the world. According to Chao et al. (2008), the volume of global accumulative water impounded by reservoirs on land has risen from about 1000 km^3 in 1950 to 11,000 km^3 in 2007, which is equivalent to an extra 30 mm of global sea level. Throughout the world, there are about 16.7 million reservoirs that have surface areas of 100 m^2 or greater (Liu et al., 2016). These reservoirs expand the global terrestrial water surface by about 305,000 km^2 (Lehner et al., 2011). Different types of reservoirs can serve a variety of applications such as flood control, agricultural/municipal/industrial water supply, and hydropower (World Commission on Dams, 2000). Of the most importance, reservoirs reduce the uneven temporal distribution in river runoff (Shiklomanov, 2000). Serving as a buffer against natural water disasters, reservoirs provide us with great convenience and flexibility in water resources management.

While reservoirs redistribute large amounts of surface water, they also dramatically alter the natural hydrological processes. Results from Graf, (2006) show annual peak discharges are decreased by 67% (on average), and daily discharge ranges are reduced by 64% due to the construction of many large dams on North American rivers. In the continental United States (CONUS), the total amount of water that can be stored by its 75,000 dams is as much as one year's mean runoff (Graf, 1999). In addition, because of dam-induced surface water area expansion, the increased water loss through evaporation

☆ *This manuscript has been co-authored by employees of Oak Ridge National Laboratory, managed by UT Battelle, LLC, under contract DE-AC05-00OR22725, and Pacific Northwest National Laboratory, managed by Battelle, under contract DE-AC05-76RL01830 with the U.S. Department of Energy. The United States Government retains and the publisher, by accepting the article for publication, acknowledges that the United States Government retains a non-exclusive, paid-up, irrevocable, world-wide license to publish or reproduce the published form of this manuscript, or allow others to do so, for United States Government purposes. The Department of Energy will provide public access to these results of federally sponsored research in accordance with the DOE Public Access Plan* (http://energy.gov/downloads/doe-public-access-plan).

* Corresponding author.
E-mail address: hgao@civil.tamu.edu (H. Gao).

http://dx.doi.org/10.1016/j.advwatres.2016.10.014
0309-1708/

from reservoirs is considerably large (Gallego-Elvira et al., 2010; Gökbulak and Özhan, 2006). These alterations increase the complexity involved with understanding the hydrological cycle.

Most reservoirs have the capability of storing water for supply purposes, mitigating floods, and/or generating energy for sustaining human societies. Of the 600 largest global reservoirs (with an integrated capacity of 5268 km^3), irrigation and/or municipal use is the main or secondary purpose for 274 reservoirs, and hydropower is the main or secondary purpose for 447 reservoirs (statistics based on Lehner et al., (2011)). Compared with extracting water directly from streams, a reservoir based water-supply system increases the supply reliability in most regions (Moy et al., 1986). However, global environmental/anthropogenic changes—such as climate change, land-cover/land-use change (LCLUC), and population growth—pose great challenges to the reservoir systems (Vörösmarty et al., 2000). More variable precipitation, constantly increasing temperatures, and more frequent floods and droughts are all threatening the sustainability of water resource management (Conway, 1996; Zhao et al., 2016). Meanwhile, water demand is increasingly driven by a fast-growing population (Oki and Kanae, 2006). To improve the adaptive capacity, more precise and spatially specific policies are needed to promote effective water use. Therefore, to better understand the intricacies of how the regulated hydrological cycle responds to complicated environmental changes—and to support the policy-making process—accurate hydrological simulations with explicit reservoir components are essential.

Two types of models are generally used to represent reservoir flow regulation effects— rainfall-runoff models, and river/watershed management models. Rainfall-runoff models focus on representing the natural hydrological processes, while river/watershed management models concentrate more on Best Management Practices (BMPs) for water uses. Many rainfall-runoff models, including the Distributed Large Basin Runoff Model (DLBRM) (Croley and He, 2005) and the Regional Hydroclimate Model (RegHCM) (Kavvas et al., 1998), do not have a reservoir component. Hydrologic models with reservoir simulation capability include the Soil and Water Assessment Tool (SWAT) (Arnold and Fohrer, 2005), the Variable Infiltration Capacity (VIC) model (Haddeland et al., 2006), and global water resources model H08 (Hanasaki et al., 2006). However, the reservoir operating schemes employed by these models are generally based on monthly generic operating rules, which are simplified such that the applications are limited to representing seasonality and inter-annual variability. Subsequently, these models are not suitable for reproducing the timing sensitive sub-monthly operational flood control activities (Voisin et al., 2013a). The role of reservoirs in the nexus of climate, energy, water, and food has been included in some recent integrated system modeling initiatives, such as the Platform for Regional Integrated Modeling and Analysis (PRIMA) (Kraucunas et al., 2015) and BioEarth (Adam et al., 2014). These models are designed to help further understand geophysical processes and their interaction with human activities at regional to sub-regional scales (operating at a spatial modeling resolution of about 12 km), in order to support decision-making. In parallel with present efforts toward hyper-resolution (e.g. less than 500 m) hydrologic modeling (Bader et al., 2014; Wood et al., 2011), in this study we explore ways to incorporate reservoir operations at fine spatial and temporal scales—which will support hyper-resolution hydrologic modeling and decision-making for local policy makers at the scale of a specific utility, reservoir(s), or watershed.

River/watershed management models typically adopt operational node-based reservoir functions. Examples of these models are the Water Evaluation and Planning System (WEAP) (Yates et al., 2005), the Hydrologic River Operations Study System (HYDROSS) (U.S. Bureau of Reclamation 1991), RiverWare (Zagona et al., 2001), OASIS software (HydroLogics Inc, 2007), MODSIM (Labadie and Larson, 2007), and the Water Rights Analysis Package (WRAP) (Wurbs, 2012). Some management models use embedded optimization algorithms to identify operating rules (e.g., WRAP), while others use predefined rules to dictate reservoir operations (e.g., RiverWare and WEAP). The river routing is either coupled with the reservoir functions (e.g., WEAP) or is conducted offline (e.g., WRAP). Because the hydrological simulations are usually lumped and parametric, these models are not appropriate to analyze the interdependence between hydrological processes and water management practices. In light of the fast environmental changes and non-stationarity conditions (e.g. climate change and LCLUC) (Milly et al., 2008), realistic representation of watershed processes is needed for effective water management decisions.

To fill in the gap between the two types of models discussed above, we present a reservoir simulation module that uses conditional rules based on observed operational and more complex operating rules. The reservoir module is similar to the reservoir operations schemes of ColSim over the Columbia River Basin (Hamlet and Lettenmaier, 1999), the Central Valley Model (CV-Mod) (VanRheenen et al., 2004) over California, and the Colorado River Reservoir Model (Christensen et al., 2004)—each of which are simplifications of applied complex offline reservoir operations management models. We integrate the reservoir module with a physically based distributed hydrologic model. More specifically, the new reservoir module is applicable to multiple reservoirs with multi-purpose flow regulations (such as hydropower water release and municipal/industrial/agricultural water supply). Although the model does not consider incoming flows over a future period, it is structured so that reservoirs share their status (storage) and conditional releases can be optimized. This new model builds upon the node-based reservoir models with complex operating rules, and adds flexibility in exploring new demand, new hydro-plants, and/or new operation rules. It also builds upon generic operating rules by being fully integrated with the hydrologic cycle. Together, the new model brings the application and decision-making capabilities from the monthly regional scale to the sub-monthly and sub-regional scales. These capabilities are crucial for understanding flow regulations in an environment that is changing in response to fine spatial and temporal resolution conditions, such as extreme climate events and LCLUC.

While the focus of this paper is mainly on the technical implementation of the integrated model, its application in a sub-basin of the Brazos River Basin is also presented. The integrated modeling framework and development of the reservoir module is first described in Section 2. A case study using the model to simulate the effects of multi-purpose reservoirs is presented in Section 3. Furthermore, sensitivity analyses (as described in Section 4) are conducted to evaluate how different designs of reservoir and input climate forcings will affect water storage and release.

2. Modeling approach

2.1. The distributed hydrology soil and vegetation model (DHSVM)

The DHSVM is an open source hydrological model that has the capability of simulating various land surface processes (Fig. 1a, b) (Wigmosta et al., 1994). It is physically based and supports high spatial and temporal resolution simulations. This model employs full water-energy balance to calculate the water partitioning within each grid cell. Specifically, the Penman-Monteith equation is used to calculate evapotranspiration (ET) from both over-story and under-story vegetation. Surface runoff and baseflow from each grid cell are first accumulated to the streams, and then routed downstream according to a Digital Elevation Model (DEM)-based river network using the linear reservoir method. DHSVM has been

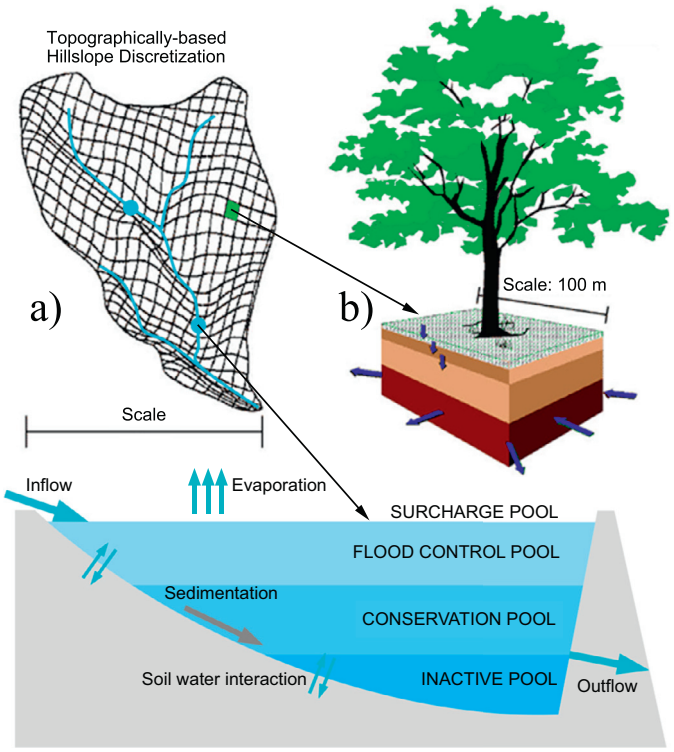

Fig. 1. Conceptual representation of DHSVM and the newly integrated multi-purpose reservoir module, which includes: (a) topographically based basin discretization in DHSVM; (b) water movement for each grid cell; and (c) the newly integrated, multi-purpose reservoir with a flood control pool, a conservation pool, and an inactive pool. Panels (a) and (b) are modified according to Wigmosta et al., (1994). Blue points in (a) represent the point reservoirs that can be simulated in the integrated model.(For interpretation of the references to colour in this figure legend, the reader is referred to the web version of this article.)

successfully applied in many research fields, including climate change (Battin et al., 2007), urbanization (Cuo et al., 2008; 2009), sediment transportation (Doten et al., 2006), glacier dynamics (Naz et al., 2014), stream temperature, and water quality simulations (Sun et al., 2015).

As a hyper-resolution model, DHSVM has the capability of simulating fast hydrologic responses (e.g., flash flood), especially over domains which are highly spatially heterogeneous. Additionally, this spatially distributed and physically-based model can be used for investigating hydrologic impacts from changing environmental conditions such as climate change and LCLUC. It should be noted that DHSVM can explicitly simulate the effects of urbanization on the hydrological regime because of its capability to represent impervious land cover and detention ponds (Cuo et al., 2008).

However, because existing versions of DHSVM can only simulate naturalized flow, the advantages of DHSVM have been greatly hindered when applied in regions where flow regulation is significant. To overcome this model limitation and leverage the model's strengths, a reservoir module was developed and fully integrated into DHSVM in this study. We expect the DHSVM-reservoir model to be used for predicting water availability over regions with notable environmental changes, and/or over regions with flood control operations which require a dynamic response.

2.2. Reservoir module

To maximize the functionality of reservoirs, most water management agencies divide their reservoirs into several pools. This approach has been well adopted worldwide, such as by the United States Army Corps of Engineers (USACE) (Wurbs, 1996), the China Ministry of Water Resources (http://www.mwr.gov.cn/), and the Central Water Commission of India (http://www.cwc.gov.in/). As illustrated in Fig. 1c, each pool is designated with a specific service objective. The surcharge pool is the part of the reservoir that is above the spillway crest. The flood control pool is right below the surcharge pool, and is regulated to reduce the regional flood risk. Regular water supply—such as that for agricultural, municipal, and industrial use—is provided from the conservation pool, which is below the flood control pool. If hydropower facilities are connected to the reservoir, the conservation pool will also be responsible for providing water to the turbines. Because inflow varies by season, it is a common practice that the top of the conservation pool is adjusted accordingly by the reservoir managers. The inactive pool (i.e., "dead storage") is the bottom portion of a reservoir that is retained to support several functionalities, such as sediment containment and ecosystem protection. In general, the top of the conservation pool is considered the optimal water level. If the current storage is maintained at this optimal level, the reservoir will have enough space to store possible incoming floodwater from upstream—and will also be able to release enough water (from the conservation pool) for various water uses.

Reservoir bathymetric information is important for assigning the pools. Generally, the storage-area and storage-elevation relationships can be depicted by tabular data, linear equations, or some non-linear equations that can better fit the observations. In this module, we defined the default option for these relationships using two exponential functions (Eqs. 1 and 2).

$$A = \alpha_A \cdot S^{\beta_A} + \gamma_A \tag{1}$$

$$H = \alpha_H \cdot S^{\beta_H} + \gamma_H \tag{2}$$

where A, H, and S are the reservoir surface area (m^2), the water elevation (m), and the storage (m^3) values, respectively; and α_A, β_A, γ_A and α_H, β_H, γ_H are the coefficients for the storage-area and storage-elevation relationships. These coefficients can be obtained by regression. The two equations can represent a wide range of relationships including convex ($\beta > 1$), concave ($\beta < 1$), or linear ($\beta = 1$) relationships. Furthermore, users have the option to characterize the bathymetry using other equations (e.g. quadratic). This is a user-defined parameterization which is specifically included for hyper-resolution modeling (and differs from large scale integrated hydrology-reservoir models, which usually provide a default shape (Fekete et al., 2010; Liu et al., 2016)).

Using the reservoir characteristics described above, a point reservoir module was developed and coupled to DHSVM. While the reservoir evaporation loss is calculated based on water surface area, the use of a point reservoir implies that the storage is not distributed over multiple grid cells but is to be managed for releases. Point reservoirs are assigned to their actual dam locations, and are jointly managed throughout the basin using conditional operating rules. There can be only one point reservoir per grid cell, and—in the case of DHSVM—one reservoir per river segment. Given the hyper-fine spatiotemporal resolution of DHSVM, the river routing was constructed using river segments that can encompass multiple grid cells for computational stability (Wigmosta et al., 1994). Forced by upstream inflow and local precipitation, outflow and storage values at each reservoir in the basin are calculated based on the release scheme and the mass balance. Fig. 2 shows the schematic of the reservoir module and its integration into DHSVM. At each DHSVM time step, the reservoir simulation involves three components: the reservoir storage evaporation scheme, the release scheme, and the reservoir storage balance calculation.

2.2.1. Evaporation scheme

Evaporation losses from open water can be considerably large, especially in arid and semi-arid regions. In this study, we used the

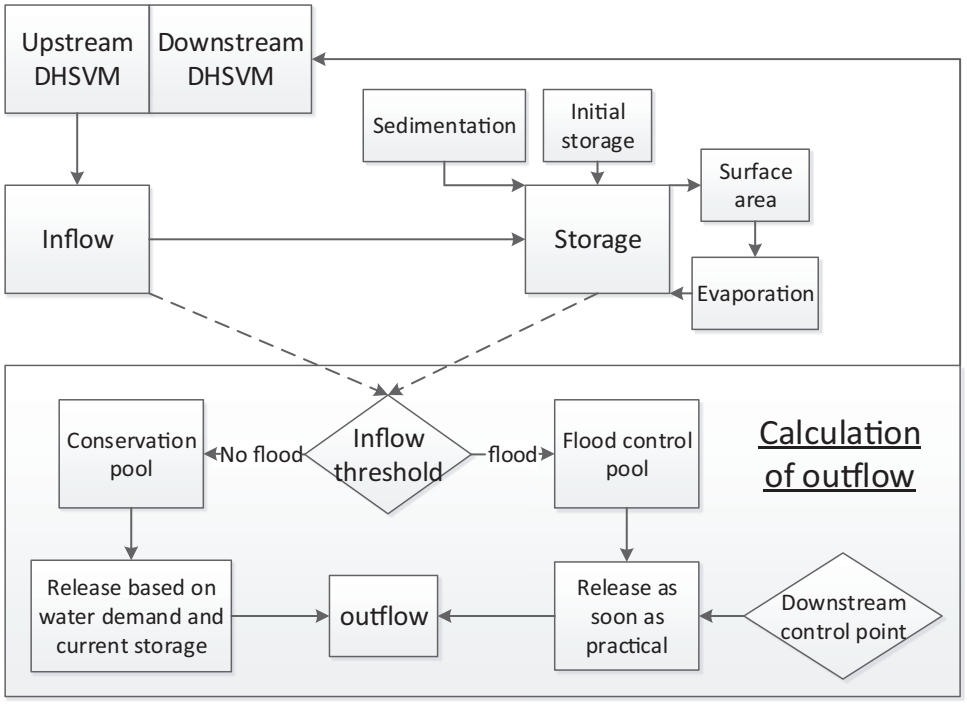

Fig. 2. Schematic of the reservoir module and its integration into DHSVM.

Penman Equation (Eq. 3) (Penman, 1948) to estimate the open water evaporation from a given reservoir:

$$E_t^o = \frac{mR_n + \rho_a c_p(\delta e) g_a}{\lambda_v(m+\gamma)} \tag{3}$$

where E_t^o is the open water evaporation rate (kg/m^2/s) at time t; m is the slope of the saturation vapor pressure curve (Pa/K); R_n is the net radiation (W/m^2); ρ_a is the air density (kg/m^3); c_p is the heat capacity of air (J/kg/K); δe is the vapor pressure deficit (Pa); g_a is the surface aerodynamic conductance (m/s); λ_v is the latent heat of vaporization (J/kg); and γ is a psychometric constant (Pa/K). Although $\boldsymbol{\lambda_v}$ depends on water temperature, we used air temperature as a substitute by assuming that surface water and surface air are in a state of temperature equilibrium, without considering the thermal stratification within the water. All of the inputs are readily available from DHSVM forcings, or are computed by DHSVM. The calculated reservoir evaporation, E_t^o, is then used in the reservoir storage water balance computations (as discussed below in the Section 2.2.3).

2.2.2. Release scheme

In the reservoir module, the water released at time t, Q_t^{out} (m^3/time step), is calculated as a function of several factors (such as upstream flow conditions, current storage values, downstream flow conditions, and water demand) using Eq. 4:

$$Q_t^{out} = \begin{cases} 0 & (H_t \le H_I) \\ U_w & (H_I < H_t \le H_C) \\ \alpha \cdot r \cdot (H_t - H_C) & (H_C < H_t \le H_F \text{ and } Q_d \le Q_{d\_max}) \\ 0 & (H_C < H_t \le H_F \text{ and } Q_d > Q_{d\_max}) \\ (S_t - S_F)/\Delta t & (H_F < H_t) \end{cases} \tag{4}$$

where H_I, H_C, H_F, S_I, S_C, and S_F are the elevation and corresponding storage values at the top of the inactive, conservation, and flood control pools, respectively (m and m^3). H_t and S_t are the real-time elevation and storage values (m and m^3). U_w is the water demand (m^3/time step), which includes multi-sectoral demand and environmental flow, and α is the flooding condition multiplier (which is equal to 1 when the inflow is not flood inflow, and is greater than 1 when the inflow is flood inflow). The threshold for determining flood inflow is a user-defined parameter, Q_f^{in}. r is the discharge coefficient (m^2/time step), which is an empirical parameter associated with the dam structure. Q_{d_max} and Q_d are the maximum acceptable streamflow and the current streamflow at downstream control points (m^3/time step), and Δt is the modeling time step (e.g., 24 hours).

As described in Eq. 4, if the real time water level in the reservoir is less than that of the inactive pool ($H_t \le H_I$), water release will not be allowed. If the water level is greater than that of the inactive pool—but less than that of the conservation pool ($H_I < H_t \le H_C$)—water release will be allocated based on the water demand (U_w). Water demand defined in the current module includes both consumptive and non-consumptive uses, including municipal, industrial, agricultural, environmental flow, and hydropower. If a reservoir is used to simultaneously meet both the hydropower generation purposes and any of the other three water supply needs, water first goes through the turbines to generate electricity as long as the release does not exceed turbine capacity. Otherwise, the excess water is released through the spillway (see Appendix A for the calculation of hydropower).

In this reservoir module, water demand (U_w) can be either prescribed or calibrated, depending on data availability. If water demand information of a specific reservoir is well documented and accessible at the modeled time step (e.g., daily), the time series data can be used directly as the reservoir module input. However, this does not apply to most of the reservoirs. To solve this problem, we provided an empirical monthly water-demand option in this module. The monthly water demand data can be either acquired from existing sources (e.g., technical reports, water-use surveys, and/or limited observations) or estimated through calibration (when information is unavailable or only partially available). The monthly data is then partitioned evenly into water demand for each modeling time step. At a global or continental scale, water demand information for each reservoir is typically derived by associating spatially distributed estimates of demand with the nearest reservoirs. This is based on a grid cell's location with respect to the reservoir (elevation, distance from

downstream impounded channel) and the reservoir's capacity (Haddeland et al., 2006; Hanasaki et al., 2006). However, the derivation of the demand can be a source of significant uncertainty in reservoir operations (Biemans et al., 2011; Voisin et al., 2013a; b).

When the water level in the reservoir is greater than that of the conservation pool—but less than that of the flood control pool ($H_C < H_t \leq H_F$)—water is evacuated as soon as practical to protect the dam. However, this release cannot exceed the maximum flow capacity of the downstream river channels (Q_{d_max}). If the downstream flow is less than the channel capacity ($Q_d \leq Q_{d\_max}$), the water release rate is calculated based on the difference in elevation between the current water level and that of the conservation pool (Eq. 4). When the upstream river basin is flooded, the flood control pool is evacuated and the flooding condition multiplier α is assigned a value greater than 1. The parameter α was first introduced by Lund and Ferreira (Lund and Ferreira, 1996) to prevent the dam from being overtopped by floods. If α is not provided for a given reservoir, users can either assign it based on experience or calibrate it against downstream flows. According to Eq. 4, if a flood event is detected downstream ($Q_d > Q_{d\_max}$), all of the reservoir gates are closed immediately—and they will remain closed until the downstream flow is under the channel capacity. Finally, in this reservoir module, when a severe flood event causes the flood control pool to be overtopped ($H_F < H_t$), the reservoir will release all of the water that exceeds its flood control capacity.

For a multi-reservoir system, water needs to be held in upstream reservoirs as much as possible to increase the flexibility of supplying water to downstream users. To implement this, our reservoir module is designed as follows: For each reservoir in the system, its water supply is first used to meet the demands (i.e., hydropower, municipal, agricultural) located in the immediate downstream river reach (but not downstream of any other reservoirs). If extra water is still available after meeting such demands, then the extra water can be allocated to reservoirs further downstream which cannot meet their own local demands (i.e., the demands from their immediate downstream river reaches). Similarly, if a given reservoir does not have enough water to meet local demands, then water will be extracted from upstream reservoirs. Thus, in this model there are multiple options for satisfying the demands of a multi-reservoir system. This process is consistent with other approaches used in coupled hydrology-routing-reservoir models (Hanasaki et al., 2006), which also use generic operating rules. In this case study, parameters associated with reservoir operating rules were calibrated (see Section 4.1) by adjusting the releases to provide downstream reservoirs with the supplies they need to satisfy their own local demands. For a complicated system, optimization is an option to achieve specific objectives (e.g., highest economic outcome). The rule of holding water in upstream reservoirs is also applicable to flood conditions. The release from an upstream reservoir needs to be stopped if its adjacent downstream reservoir is crested. However, if the upstream reservoir water level is above the flood control pool, water will be released. Both cases are described in Eq. 5,

$$Q_t^{out} = \begin{cases} 0 & (H_t^{DR} > H_F^{DR} \text{ and } H_t \leq H_F) \\ Q_t^{out} & \left(H_t^{DR} \leq H_F^{DR}\right) \end{cases} \quad (5)$$

where H_t^{DR} and H_F^{DR} are the downstream reservoir real-time elevation and flood control pool elevation values, respectively.

In large-scale integrated hydrologic modeling, the caveat for generic reservoir operating rules is that they do not allow for joint management among reservoirs (Hanasaki et al., 2006). However, basin-specific case studies, which provide more information about joint management practices, allow for simulations of joint operating rules among reservoirs (e.g., for flood control) (Mateo et al., 2014). Offline optimization of reservoir operations is also possible in large-scale modeling, although it increases the computational burden—and still results in a simplified regulation system in which only major reservoirs are represented (Haddeland et al., 2006; Zhou et al., 2016). In operational basin-scale reservoir management, multiple sets of optimized seasonal to inter-annual operating rule curves are available—and the selection of the optimum set is based on a projection of seasonal inflow into the reservoir. This insight is usually available when the reservoir model is run offline of the hydrology model, with a time series of naturalized inflow into the upstream reservoir (and the contributing segments) provided. Because those reservoir models are offline, 2-way coupling and the representation of interdependencies (between the hydrology model and the river routing and reservoir models) are limited. In this study, we chose to better represent the above mentioned interdependencies (by implementing a reservoir module into the DHSVM hydrologic model), while using a compromised choice with regard to the optimum set of operating rules (e.g., the release decision has no insight on the future inflow). The implementation of this reservoir module within DHSVM (with fully coupled hydrology, river routing, and reservoir processes) is compatible with future applications involving the coordination of reservoirs through the optimization of the empiric release rules. However, the computational burden of the hydrology part remains, and therefore the future optimization of DHSVM reservoir operations will need to be accompanied by computational changes such as parallel processing.

2.2.3. Reservoir storage calculation

Considering the mass balance, Eq. 6 is used to represent the change in reservoir storage:

$$S_t = S_{t-1} + \Delta t \cdot \left(Q_t^{in} - E_t^o \cdot A_t - Q_t^{out} - \Delta_{sed}\right) \quad (6)$$

where Q_t^{in} *and* Q_t^{out} are the inflow and release values (m^3/time step); E_t^o is the open water evaporation (which is calculated in Eq. 3, m^3/time step); Δ_{sed} is the sedimentation rate (m^3/time step); and Δt is the time step.

Sedimentation, which is caused by the trap efficiency (TE) of the dams (Brune, 1953), is an important process within a given reservoir. It reduces the reservoir storage capacity by gradually accumulating the sediment from upstream inflows and from the surrounding areas. According to Mahmood (1987), one percent of the total storage capacity in global reservoirs is filled by sediment every year. In this module, we introduced a sedimentation parameter to account for this impact (Δ_{sed}). A detailed description of the parameters used in this module is provided in Appendix A. Even though our reservoir module can also be integrated into other simpler and coarser (or even statistical) watershed models, the implementation is customized to the hyper-resolution hydrology model DHSVM for two reasons. First, although the difference between a simpler/coarser model and a fully distributed physically based model (e.g., DHSVM) may be very small for a relatively homogeneous large watershed at a low temporal resolution (e.g., monthly), a simpler model is unlikely to accurately represent highly spatially heterogeneous land cover and/or to accurately simulate flows at fine time steps. Second, DHSVM can provide a full set of input data to the reservoir module, which allows the module to accurately represent all of the attributes involved in the operations (e.g., flood control, evaporation from reservoir, sedimentation, and (future) water temperature).

2.3. Model integration

The point reservoir module is integrated into the DHSVM routing scheme to represent reservoirs at their real locations (instead of lumping them together at basin/subbasin outlets). Meanwhile, multiple reservoirs can be simulated simultaneously as part of the channel routing process. In the latest version of DHSVM, the river channels are represented by connected river segments,

and the routing is executed according to the order of the segments. However, by adding the point reservoirs, the connected segments (where the dams are located) are divided into upstream and downstream sections. To represent the reservoir regulation effects, DHSVM was modified as follows: (1) If the routed flow reaches a segment where a point reservoir is located, the reservoir receives inflow from the upstream section. (2) Reservoir storage and release at the current time step is then determined according to the operation rules, previous storage values, evaporation, release amounts, and sedimentation rates (Fig. 2, Eq. 6). In addition, the reservoir module examines the streamflow from the downstream controlled river segments and then modifies the release scheme accordingly. (3) Released water enters the routing network at the downstream section. After computing the reservoir release amounts, downstream water users can extract water from specified downstream river segments. This is implemented by specifying the locations (i.e., the given river segments) and amounts of extracted water in the module. Similar to the reservoir water demand data, water extraction data can also be input as time-series or empirical monthly values at the segments of interest. Extracted water can be used for multiple purposes including agricultural, municipal, industrial, and others. In the current module version, non-point return flow is not accounted for, and only consumptive use is extracted. However, point return flow may enter the river network at any location (either the same as the extraction location, or somewhere else). For instance, a drinking water treatment plant (water user) and a wastewater treatment plant (water contributor) could both be simulated in the module. In this application, the water demand is prescribed and it has combined the information such as consumptive use, irrigation technologies, and delivery efficiencies. Return flow, and groundwater dynamics associated with pumping, will need to be developed during future work. Implicit return flow and groundwater components are currently being developed within certain existing water management (WM) models (Voisin et al., 2015). A future 2-way coupling between the WM and hydrology models would explicitly address i) the redistribution of withdrawn water onto crop covered grid cells as an additional forcing, and ii) groundwater dynamics when WM is coupled to models (like DHSVM) with water table dynamics and lateral flow.

The integrated model can be executed on any Linux/Unix system with a C language compiler. Due to the high spatiotemporal resolution of DHSVM, significant computational capability is needed to run this integrated model (even though the reservoir module only adds to the running time slightly). However, users can reduce the modeling time by dividing the study sites into multiple parts. Thus, even though the integrated model is better when used at a watershed scale (due to computational expense), it can also be employed at a basin scale by dividing the basin into multiple watersheds (sub-basins) which can be simulated simultaneously using high performance computing capabilities (Zhao et al., 2016).

3. Integrated model application: case study over the Lake Whitney watershed

3.1. Study area

The Lake Whitney watershed (Fig. 3) is located in the middle of the Brazos River Basin, which is the second largest river basin in Texas. The total area of the Lake Whitney watershed is 5290 km^2, and its elevation ranges from 125 to 454 m. Besides Lake Whitney (a USACE reservoir with a capacity of 2.59×10^9 m^3), there are three other lakes/reservoirs in this watershed —Squaw Creek reservoir, Lake Pat Cleburne, and Aquilla Lake. The main purpose of the Squaw Creek reservoir (with a capacity of 1.87×10^8 m^3, about 7% the size of Lake Whitney) is to provide cooling water for the Comanche Peak Nuclear Power Plant. Lake Pat Cleburne (with

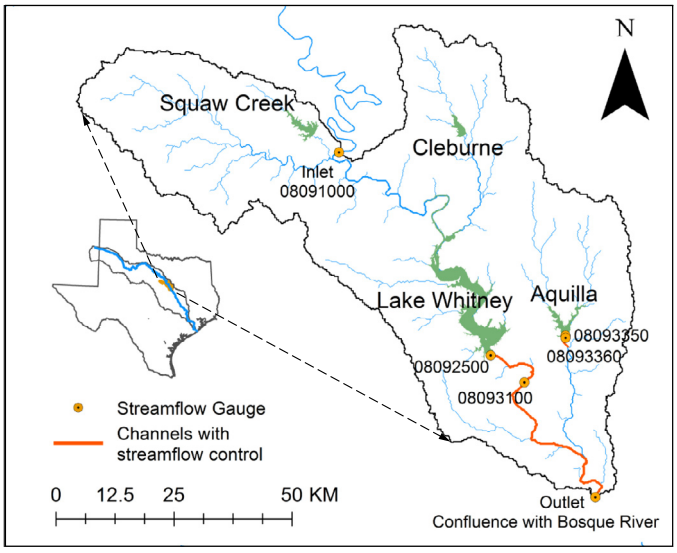

Fig. 3. The Lake Whitney watershed in the Brazos River Basin, Texas. The confluence of the Brazos River with the Bosque River was chosen as the outlet, and U.S. Geological Survey (USGS) Gauge 08091000 was chosen as the inlet. The streamflow from Lake Whitney to the outlet is restricted to under 708 m^3/s, and to under 85 m^3/s for Aquilla Lake. (For interpretation of the references to colour in this figure legend, the reader is referred to the web version of this article.)

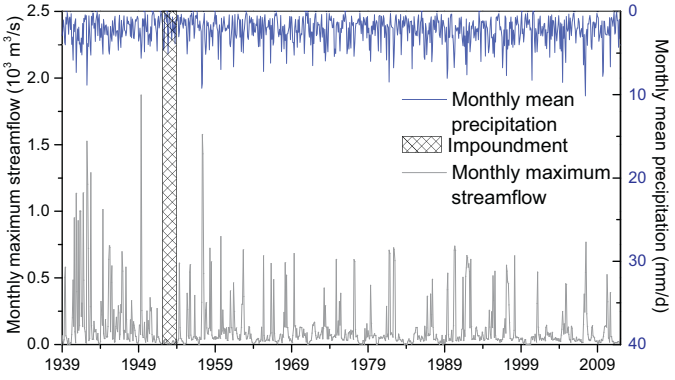

Fig. 4. Monthly maximum streamflow observations (USGS Gauge 08093100) at the downstream channel of Lake Whitney. The blue line shows the monthly mean precipitation in the Lake Whitney watershed. (For interpretation of the references to colour in this figure legend, the reader is referred to the web version of this article.)

a capacity of 3.21×10^7 m^3, which is about 1% the size of Lake Whitney) is owned and managed by the City of Cleburne (population 29,377 in 2010) to provide water for municipal uses. Aquilla Lake (with a capacity of 2.64×10^8 m^3, about 10% the size of Lake Whitney) is also managed by the USACE as a part of the Brazos River Basin flood control project. Compared to Lake Whitney, storage variations over the Squaw Creek reservoir and Lake Pat Cleburne are so small that their alteration of the streamflow can be ignored. Therefore in this study, we chose to focus on modeling Lake Whitney and Aquilla Lake.

As the largest of all 28 reservoirs (by storage capacity) in the Brazos River Basin, Lake Whitney (Fig. 3) plays an essential role in water resources management in central Texas. Whitney Dam was constructed during the period from May 1947 to April 1951, followed by deliberate impoundment. The main purpose of this reservoir is to prevent the flooding of downstream areas. It is also used for hydropower generation, municipal and industrial water supply, and recreation.

Since the construction of the Lake Whitney Dam, the natural streamflow in the downstream areas of the Brazos River has been altered significantly (Fig. 4). After the impoundment, downstream

averaged monthly maximum flow decreased from 213.79 m^3/s (USGS Gauge 08093100, from October 1938 to November 1951) to 108.74 m^3/s (from January 1954 to December 2014). The presence of Lake Whitney has significantly reduced the downstream flood risk. The only exception occurred in May 1957, when southern and central Texas experienced catastrophic floods. And even though Lake Whitney was forced to release more water because its flood pool was full, it prevented the downstream area from suffering more severe flood damage. Fig. 4 also shows that—even on a monthly scale—the precipitation variability is still quite large, which adds to the necessity of efficient reservoir operations. Meanwhile, the annual evaporation of Lake Whitney is about 2.47×10^8 m^3, which is about one-third of the conservation pool volume.

Aquilla Lake is a relatively small lake in the Lake Whitney watershed. It was impounded deliberately in April 1983, shortly after the construction of the Aquilla Lake Dam (from March 1982 to January 1983). It is part of the flood control project in the Brazos River Basin. Besides flood control, other purposes of Aquilla Lake include water supply and recreation.

Historically, Lake Whitney and Aquilla Lake have significantly contributed to water resources management in this region. However, under the impacts of future climate change (such as extreme events), there is an increasing concern about the resilience of these lakes in terms of flood control, water supply, and hydropower generation. In addition, the operation rules–which were made based on an assumption of historical stationarity —need more quantitative evaluation and are subject to change (Milly et al., 2008). The investigation of non-stationarity (of a non-linear nature) in integrated natural and human systems to support adaptations was the overall motivation for the development of this integrated model. Therefore, we use the modeling results and analysis over Lake Whitney to answer some important water management questions, such as: 1) How will climate change induced extreme events affect the current water management practices and hydropower generation? 2) Is there a need for adapting current operation rules to a changing climate, and (if so) how to go about this? Furthermore, an integrated model such as this will help us to better evaluate the need for constructing more reservoirs in a given river basin (for increasing water availability)—or, conversely, for removing outdated reservoirs in an attempt to restore the natural ecosystem.

3.2. Model input data

Inputs for the integrated model include three categories—hydrologic parameters, reservoir configurations, and meteorological forcings—as described below.

3.2.1. Hydrologic parameters

Hydrologic parameters include elevation, soil, and vegetation characteristics. The DEM was obtained from the Shuttle Radar Topography Mission (SRTM) (Jarvis et al., 2008) and was resampled to 200 m (i.e. to the DHSVM model resolution). Flow directions, basin mask, soil depth, and stream network were generated from the DEM using Arcinfo Workstation tools. The land-cover map was downloaded from the National Land Cover Database (NLCD) Multi-Resolution Land Characteristics Consortium (MRLC) website (http://www.mrlc.gov/). Because there was little LCLUC in the Lake Whitney watershed during the past several decades, NLCD 2001 (Homer et al., 2007) was used for the entire simulation period. In the Lake Whitney watershed, the main land-cover type is native grass, which accounts for 55% of the entire area. The rest of the watershed is covered by conifer forest (15%), mixed/deciduous forest (10%), urban area (8%), and other land cover types (12%). Soil texture information was acquired from the STATSGO2 database (Soil Survey Staff, 2016). The dominant soil type is clay loam (47%), followed by clay (25%), and sandy loam (19%).

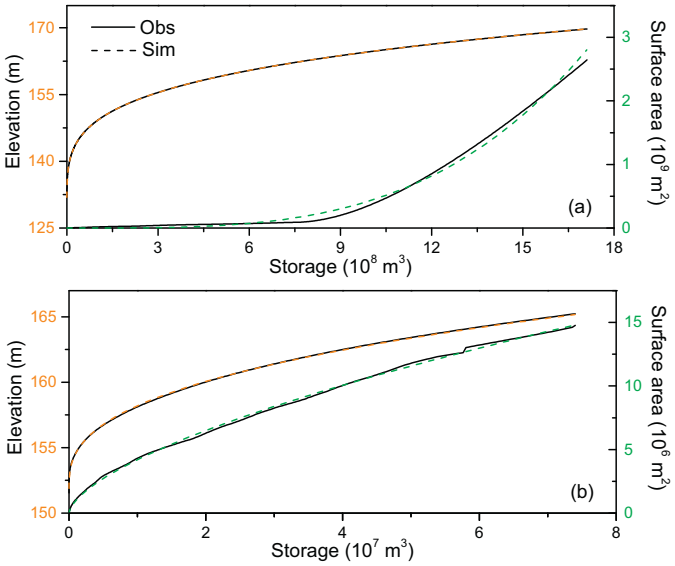

Fig. 5. Fitted storage-area and storage-elevation relationships according to observations at a) Lake Whitney; and b) Aquilla Lake. (For interpretation of the references to colour in this figure legend, the reader is referred to the web version of this article.)

3.2.2. Reservoir configurations

Reservoir storage, elevation, and surface area data were obtained from the Texas Water Development Board (TWDB) to derive the rating curves for Lake Whitney and Aquilla Lake. The coefficients in Eqs. 1 and 2 were estimated through regression. For Lake Whitney, the coefficients of determination (R^2) for these two relationships are 0.999 and 0.995, respectively (Fig. 5a). The corresponding R^2 values for Aquilla Lake are 0.998 and 0.996, respectively (Fig. 5b).

For both reservoirs, the pertinent operational data were acquired from the USACE. The Lake Whitney storage capacity (2.59×10^9 m^3) was divided into the surcharge pool (1.11×10^6 m^3), the flood control pool (1.69×10^9 m^3), the conservation pool (7.68×10^8 m^3), and the inactive pool (5.27×10^6 m^3) (Table 1). The lake surface area is 95.34 km^2 when its water level is at the top of the conservation pool. The dam has a power generation rate of 30,000 KW/hr at capacity, and its average annual power production (from 1953 to 2005) is 73 million kilowatt-hours (TWDB, 2006).

In addition to reservoir water level, flows at downstream control points are examined at each time step to decide whether water should be released (after Eq. 4). For Lake Whitney, two downstream control points are designated by the USACE. Among these two, Control Point 1 (located at the confluence of the Brazos River and the Bosque River, as shown in Fig. 3) is closest to the reservoir and has the minimum capacity of channel streamflow (amongst the two) of 708 m^3/s. Control Point 2, National Weather Service (NWS) Gauge WBAT2, is located 64 km downstream of the reservoir and has a minimum channel streamflow capacity of 1700 m^3/s. Control Point 1 was selected as our outlet to represent downstream flow-control operations. This is based on the historical experience that a full load at Control Point 1 (708 m^3/s) tends to occur more often, in which case the release from Lake Whitney will shut down long before Control Point 2 reaches its capacity. In fact, the flows at Control Point 2 have always been much less than its capacity threshold over the past 50 years (with a maximum value of 1215.60 m^3/s occurring on May 17, 1965). With respect to sedimentation, the survey conducted by the TWDB in June 2005 suggests that the conservation volume of Lake Whitney has decreased by 11.6% during the past 50 years (with the sedimentation rate being about 1.91×10^6 m^3/yr) (TWDB, 2006).

Table 1
Reservoir configuration of Lake Whitney and Aquilla Lake.

Reservoir	Lake Whitney	Aquilla Lake
Impoundment Date	December 10, 1951	April 29, 1983
Downstream control point	Confluence of Brazos River and Bosque River	Discharge gate of Aquilla Lake
Downstream controlled streamflow (m^3/s)	708	85
Sedimentation rate (m^3/year)	1.91×10^6	1.91×10^5

	Storage (accumulative, m^3)	Elevation* (m)	Storage (accumulative, m^3)	Elevation (m)
Inactive pool	5.27×10^6	136.79	1.15×10^6	155.45
Conservation pool	7.73×10^8	162.46	6.46×10^7	163.83
Flood control pool	2.47×10^9	174.04	1.80×10^8	169.47

* Elevation is measured at the top of each pool.

Table 2
Simulation error statistics (calculated on a daily, weekly, and monthly basis) for Lake Whitney and Aquilla Lake.

Lake	Variable	Time Step	Obs. Mean	Sim. Mean	Relative bias	R^2	NSE
Lake Whitney[a]	Storage[1] (10^8 m^3)	Daily	5.94	6.23	4.9%	0.87	0.72
		Weekly	5.94	6.23	4.9%	0.87	0.73
		Monthly	5.94	6.23	4.8%	0.88	0.77
	Release[2] (m^3/s)	Daily	41.26	37.94	-8.0%	0.75	0.74
		Weekly	41.26	37.94	-8.0%	0.82	0.81
		Monthly	41.20	37.89	-8.0%	0.93	0.92
	Hydropower (MWh)	Monthly	4494	3951	-12.0%	0.80	0.68
Aquilla Lake[b]	Storage[3] (10^8 m^3)	Daily	0.52	0.50	-3.3%	0.83	0.77
		Weekly	0.52	0.50	-3.3%	0.83	0.77
		Monthly	0.52	0.50	-4.2%	0.85	0.79
	Release[4] (m^3/s)	Daily	2.38	2.69	13.1%	0.54	0.51
		Weekly	2.38	2.69	13.1%	0.70	0.51
		Monthly	2.38	2.72	14.3%	0.70	0.63

1,2,3,4 Observation data from USGS Gauges 08092500, 08093100, 08093350, 08093360, respectively.
[a] Error statistics were calculated from 1950 to 2011.
[b] Error statistics were calculated from 1983 to 2011.

Aquilla Lake has a capacity of 2.64×10^8 m^3, including the surcharge pool (8.35×10^7 m^3), the flood control pool (1.15×10^8 m^3), the conservation pool (6.35×10^7 m^3), and the inactive pool (1.15×10^6 m^3) (Table 1). To reduce the downstream flood risk, outflow from Aquilla Lake is controlled to under 85 m^3/s. The sedimentation rate of Aquilla Lake is approximately 1.91×10^5 m^3/yr (TWDB, 2009).

3.2.3. Meteorological forcings

The Long-Term Hydrologically Based Dataset (1915–2011) (Livneh et al., 2013; 2015) was used to drive the integrated model. This data set covers the CONUS at 1/16° spatial resolution. The daily data set contains four meteorological variables: precipitation, maximum temperature, minimum temperature, and wind speed. The same approach from Livneh et al., (2013) was employed to obtain the other meteorological inputs for DHSVM (i.e., relative humidity, incoming shortwave radiation, and incoming longwave radiation). Specifically, the 1/16° resolution forcings were downscaled to the modeling resolution (i.e., 200 m) using the Cressman interpolation method in DHSVM (Wigmosta et al., 1994).

4. Results and discussions

4.1. Calibration and validation results

Two sets of parameters need to be calibrated: soil and vegetation parameters associated with the original DHSVM model, and reservoir parameters for the reservoir module. Because inflows into the two reservoirs are not regulated, the soil and vegetation parameters for the watershed were calibrated against inflow observations made by the USACE Fort Worth District (http://www.swf-wc.usace.army.mil/). The calibrated soil parameters include hydraulic conductivity, maximum infiltration rate, and porosity. Vegetation parameters include the Leaf Area Index, the canopy attenuation coefficient, and the maximum/minimum stomatal resistance. The reservoir module parameters are the discharge coefficient and the flood inflow threshold. Because water-demand data by category (e.g., municipal, hydropower) are not completely available for both reservoirs, the empirical monthly water demand for each reservoir was calibrated and then evenly partitioned into daily demand in this case study. The relative bias, R^2, and the NSE between the daily observations and the modeled results were used as the objective functions. These statistical variables were also used to validate the model performance.

For Lake Whitney, the model was calibrated from January 1, 2001 to December 31, 2011 and validated from December 10, 1951 (impoundment) to December 31, 2000. Fig. 6 suggests that the integrated model was able to reconstruct observed flow and storage variations reasonably well, including the impoundment in the 1950s and the change of conservation level in the 1960s. Both the R^2 and NSE values in Table 2 indicate that the model performed robustly at the multi-decadal scale. For reservoir elevation and release at Lake Whitney, the weekly R^2 values were 0.87 and 0.82, while the weekly NSE values were 0.73 and 0.81. With regard to downstream flows, the respective weekly R^2 and NSE values for USGS Gauge 08093100 were 0.82 and 0.81.

According to USACE records, the conservation pool of Lake Whitney has been adjusted three times in history. In March 1968, its elevation (blue dashed line in Fig. 6b) was raised from 158.50 m to 159.11 m, which later increased to 159.41 m in March 1969. In May 1972, it was raised to its current level (i.e., 162.46 m). The effects of this conservation pool adjustment on reservoir water level can be clearly observed in Fig. 6b.

Simulated hydropower generation results (for Lake Whitney) were also validated by comparing them with US Energy Information Administration (EIA) hydropower net generation data (http://www.eia.gov/electricity/; Fig. 6d). The R^2 value, which is equal to 0.80, shows good correlation. The disparity is partially due to the adoption of monthly averaged hydropower water releases in the case study, when in reality this varies on a daily basis. This

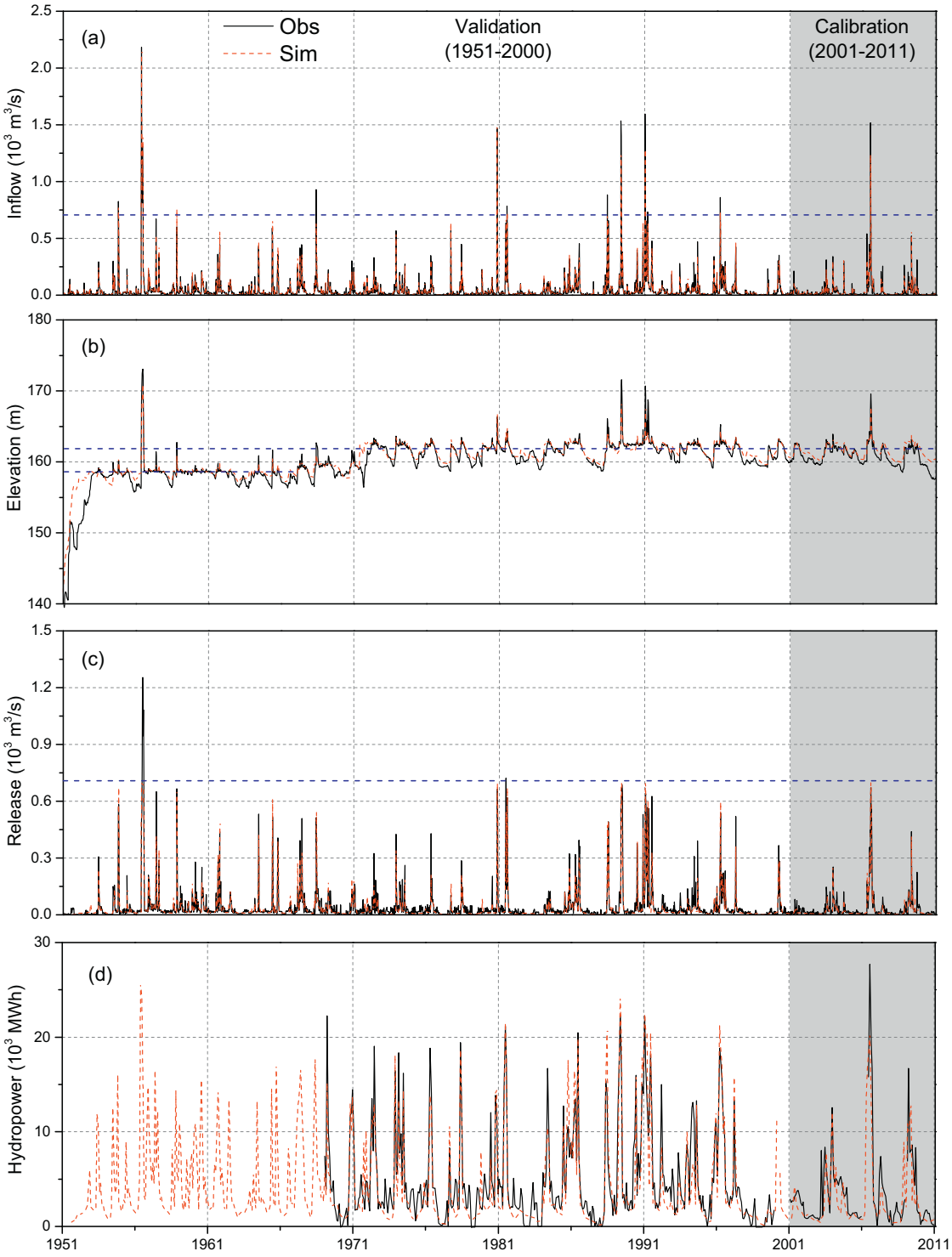

Fig. 6. Calibration and validation results for Lake Whitney: (a) inflow (weekly); (b) elevation (weekly); (c) release (weekly); and (d) hydropower generation (monthly). Blue dashed lines represent the downstream channel capacity in (a) and (c), and the top of the conservation pool in (b). (For interpretation of the references to colour in this figure legend, the reader is referred to the web version of this article.)

can be improved by considering the sub-daily, daily, and weekly hydropower demand and scheduling in the future study (which would require further sub-daily hydropower generation data, and a more in-depth hydropower module). Nevertheless, long-term generation characteristics can be captured through the current integrated modeling approach.

Because the Aquilla Lake Dam was built in 1983, the calibration and validation were conducted from 2008 to 2011 and from 1983 to 2007, respectively (Fig. 7). The R^2 values for storage and release were 0.83 and 0.70, and the weekly NSE values were 0.77 and 0.51. The daily R^2 and NSE values were lower than the weekly and monthly values because water supply data for calibrating the monthly demand were not available for this reservoir.

4.2. Effects of Lake Whitney on peak and low flows

The effect of reservoirs in mitigating flood peaks was also explored by comparing the simulated inflows and releases for Lake

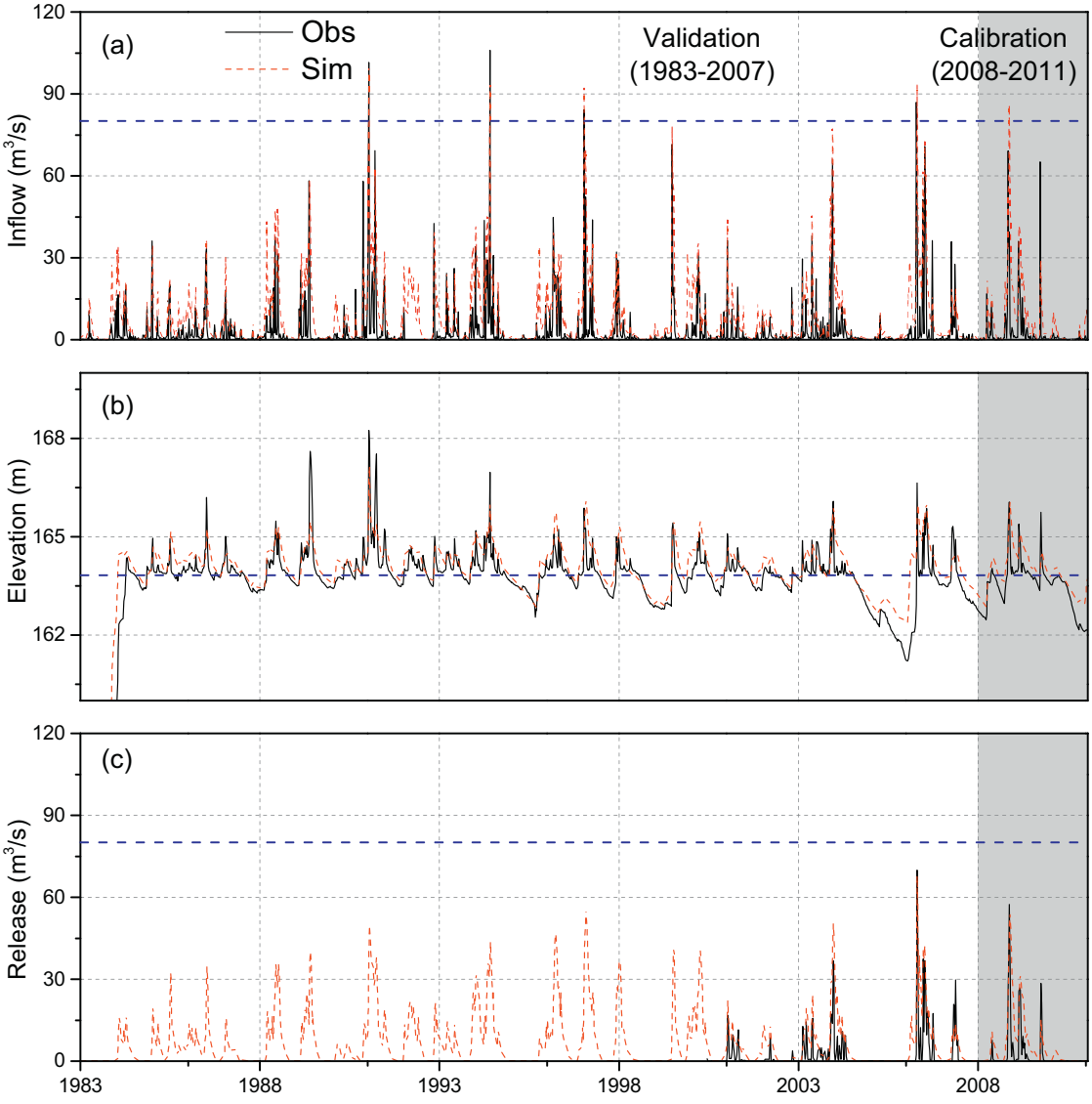

Fig. 7. Weekly calibration and validation results for Aquilla Lake (a) inflow; (b) storage; and (c) release. Blue dashed lines represent the downstream channel capacity in (a) and (c), and the top of the conservation pool in (b). (For interpretation of the references to colour in this figure legend, the reader is referred to the web version of this article.)

Whitney. Because point reservoirs were used in the integrated model, the inflow to a given reservoir can be roughly regarded as the unregulated/naturalized outflow without the reservoir. Thus, differences between inflows (Fig. 6a) and releases (Fig. 6c) reflect the influence of Lake Whitney on flow regulation. Here we use statistical analysis of the simulated peak flows and low flows during the period of 1953 to 2011 to explain the impact of reservoir regulation. The averaged monthly maximum streamflow is 76 m^3/s with Lake Whitney regulation included, while the value is two times larger (235 m^3/s) when only considering natural flow. In contrast, the low flow – represented by the lowest 7-day average flow that occurs (on average) once every 10 years (7Q10) – is 0.45 m^3/s with the reservoir, and 0.37 m^3/s without the reservoir. These results clearly show the capability of Lake Whitney in mitigating both floods and droughts.

In this study, we chose the flow from 1980 to 1985 as a representative to illustrate the reservoir impacts (Fig. 8). Using the flood event in October 1981 as an example (Fig. 8b), maximum inflow was 1471 m^3/s in the week of October 14. If this streamflow had been directly routed downstream with no reservoir, a huge flood event would have occurred because the downstream channel capacity would have been exceeded by about 700 m^3/s. With flood control at Lake Whitney, the release was reduced to 708 m^3/s.

As compared to peak flows–which are mainly affected by dam operations–low flows are primarily driven by downstream water users. As explained in Section 2.2.2, model users have several options for incorporating information about water demand. In the case of Lake Whitney, hydropower water use is dominant. Thus, the released low flow mainly depends on hydropower water demand. We selected the low flow event that occurred from 1982 to 1984 as an example to show the impacts of reservoir operation on low flows (Fig. 8c). Compared with naturalized flow (inflow), the release shows significantly improved stability which increases the water supply reliability at the study site.

Thus, with the new module, the major added value is the reservoir storage simulation, which incorporates water use and reservoir operations. Without the reservoir module, it can be very difficult to assess water availability and flood risks. Along with better simulated streamflow, the integrated DHSVM can now be used in watersheds that have flow regulation activities. In addition, the integrated model provides the important capability of simulating detailed hydrology and water management practices simultaneously.

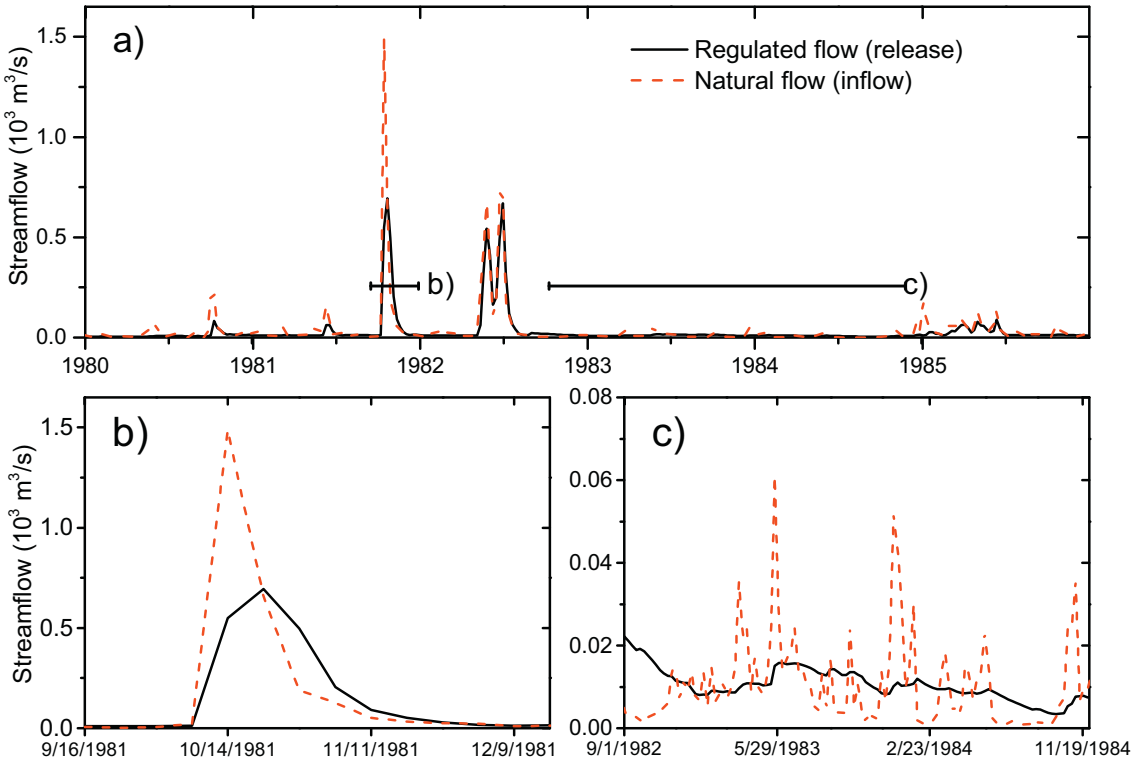

Fig. 8. Impacts of reservoir operations on streamflow. Particularly, a peak flow event in 1981 (panel b) and a low flow event from 1982 to 1984 (panel c) were selected out for better illustration.

This characteristic can be used for further exploration of the interdependence of these two systems.

4.3. Model parameter sensitivity analysis

The integrated modeling framework provides a unique benefit for conducting comprehensive sensitivity tests of the reservoir parameters (which represent the operation rules). Given the same hydrologic conditions, the effects of flow regulation depend on the selection of the reservoir parameters. Insufficient water storage will plague the reservoir ecosystem, hydropower, and recreation, while excessive amounts of water in a reservoir will increase the risk of dam fracturing and downstream flooding. Thus, in this study, a series of parameter sensitivity analyses were conducted for reservoir storage and downstream flows. In addition, the sensitivity analyses also help to quantify the uncertainties associated with the module parameters. We demonstrate the results from Lake Whitney, which has a much larger socio-economic and environmental impact than Aquilla Lake. Among all reservoir parameters (as listed in Appendix A), reservoir storage and release are the most sensitive to the following four inputs in our current model configuration: monthly hydropower water demand (MHWD; the amount of water that needs to be released to the turbines in order to provide hydropower), flood inflow threshold (FIT; Q_f^{in} in Section 2.2.2) to determine if inflow is a flood inflow, conservation pool storage (CPS; S_C in Eq. 4), and a discharge coefficient related to the dam structure (DC; r in Eq. 4). Fig. 9 shows the sensitivity test results of storage and release (peak, mean, and low) to these parameters. Analysis of the sensitivity of reservoir storage and release was performed by changing the calibrated value of these parameters by $\pm 10\%$, $\pm 20\%$,and $\pm 50\%$— except in the case of CPS, which was changed by the order of $+20\%$ to -20%.

Results indicate that MHWD has a significant inverse correlation with storage. If MHWD is reduced by 50%, average storage will correspondingly increase by 3.9% (Fig. 9a, non-shaded area). However, because peak release is mostly affected by flood events while low release is influenced by environmental control flow, the impact of MHWD on release was insignificant in this study (Fig. 9a, shading area). FIT has a very small effect on both storage and release (a -50% change produces a 0.2% storage increase and a 0.3% release decrease, and a 50% change yields a 0.1% storage decrease and a 0.3% release increase; Fig. 9b). This is because in the integrated model—even though the use of the flood control pool depends on whether the inflow is greater than the FIT—real-time release values are only based on the current storage conditions. For instance, if the current water level is above the top of the conservation pool but—at the same time—the simulated inflow is less than the IT, the reservoir will still need to release water quickly in order to drop the water level. Our analyses suggest that CPS is the parameter that both the storage and release are most sensitive to (Fig. 9c). A reduction of 20% CPS results in a 12.2% decrease in storage volume and a 12.6% increase in release. In contrast to the small effect on storage, the release is more sensitive to changes in model parameter values (as reflected by large variations of peak, mean, and low outflows). Peak release turned out to be most sensitive to CPS; a 20% decrement of CPS resulted in a 14.44 m^3/s (21.7%) increase of peak release. In contrast, a 20% decrement of CPS only reduced the low release by 0.37 m^3/s (2.5%). This is because when CPS is reduced, more water is released during flood events. For DC, clear nonlinearity can be observed (Fig. 9d). In the -20% to 50% range, there is little change in storage and release values. But when DC was decreased by -50%, reservoir storage volume dramatically increased and release volume dramatically decreased.

4.4. Sensitivity to precipitation and temperature changes

In addition to their sensitivity to model parameters (determined by operation rules), storage and release values are also sensitive to the meteorological forcings. Precipitation intensity can vary greatly over different spatial/temporal domains. Moreover, because of the impact of climate change and decadal oscillations such as the El

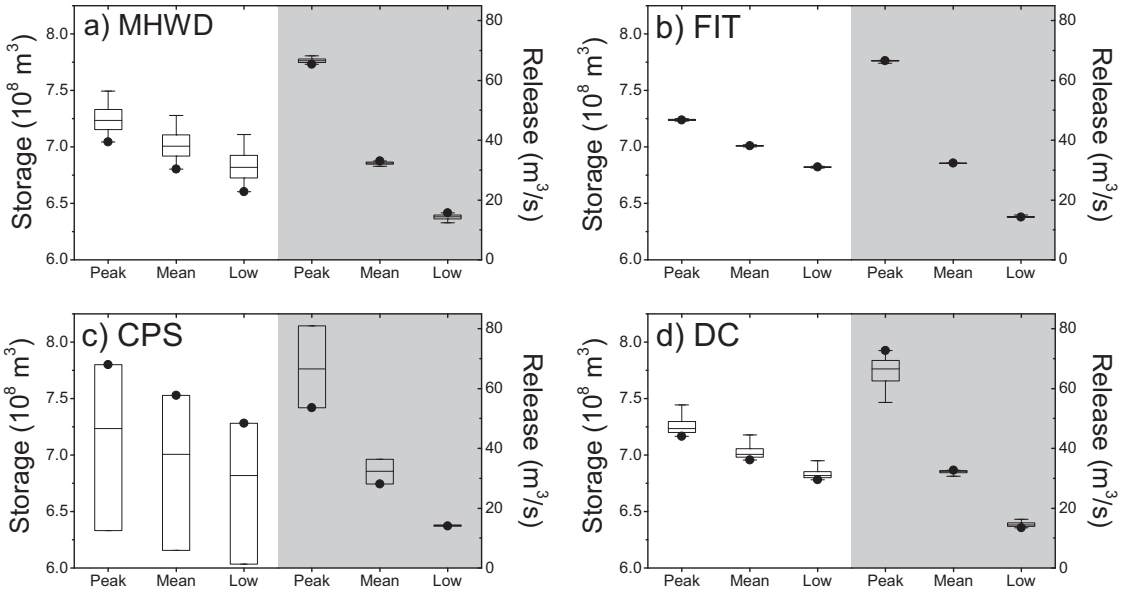

Fig. 9. Sensitivities of reservoir storage (non-shaded area) and release (shaded area) to (a) monthly hydropower water demand; (b) flood inflow threshold; (c) conservation pool storage (with −20% to +20% variability); and (d) discharge coefficient. The middle bar is the result using the calibrated parameter value. The box represents the results using the parameter when perturbed from −20% to +20%. The whisker represents the results using the parameter perturbed from −50% (without dots) to +50% (with dots). Peak/Low storage was calculated by averaging the monthly maximum/minimum storage. Low release flow was defined as the minimum 3-day streamflow, while peak release was calculated by averaging the monthly maximum release.

Niño Southern Oscillation (ENSO), variability of precipitation is very likely to increase (Seager et al., 2005). Such increased variability clearly aggravates the complexity of water resources management in reservoir systems (Christensen et al., 2004; Gutierrez and Dracup, 2001; Milly et al., 2008). According to the Intergovernmental Panel on Climate Change (IPCC) Fifth Assessment Report (Stocker et al., 2013), global temperature is projected to be 3.7 °C higher at the end of the 21st century globally than the 1986–2005 average under Representative Concentration Pathways 8.5. This increase of temperature will result in a higher evapotranspiration rate, which will subsequently affect other water budget terms. Therefore, it is necessary to evaluate how reservoir systems will respond to changes in precipitation and temperature.

In this study, storage and release were examined for each season in terms of precipitation elasticity and temperature sensitivity. Precipitation elasticity of release ($\varepsilon_P(P, Q)$), as defined in Eq. 7, is commonly used to estimate how the streamflow will change based on changes of precipitation (Sankarasubramanian et al., 2001; Schaake, 1990). To evaluate the effect of precipitation on storage, we defined the precipitation elasticity of storage, $\varepsilon_P(P, S)$ (Eq. 8). Similarly, temperature sensitivity of release (Nash and Gleick, 1991), $S_T(P, Q)$, and temperature sensitivity of storage, $S_T(P, S)$, were defined in Eqs. 9 and 10, respectively. Here, the unit for Q and P is m^3/s and mm/day, while the unit for T is °C.

$$\varepsilon_P(P, Q) = \frac{\Delta Q/Q}{\Delta P/P} \tag{7}$$

$$\varepsilon_P(P, S) = \frac{\Delta S/S}{\Delta P/P} \tag{8}$$

$$S_T(P, Q) = \frac{\Delta Q/Q}{\Delta T/T} \tag{9}$$

$$S_T(P, S) = \frac{\Delta S/S}{\Delta T/T} \tag{10}$$

Results from Fig. 10a-b indicate that both $\varepsilon_P(P, Q)$ and $\varepsilon_P(P, S)$ will increase as precipitation increases. The range varies from 0.09 to 0.19 for storage and 0.66 to 1.68 for release. However, the precipitation elasticity is not always linearly correlated with the percentage of change in precipitation. For example, $\varepsilon_P(P, S)$ keeps increasing from a −30% to a 10% change in precipitation, but then remains constant from 10% to 30%. The increase in $\varepsilon_P(P, Q)$ indicates that an additional unit increase of precipitation will result in a larger increase of release. Eventually, the rise in inflow will cause the water level in the reservoir system to rise. However, because the optimal water level is defined by the CPS, reservoir managers need to release the excess water as soon as practical. This leads to limited growth of $\varepsilon_P(P, S)$ when $\Delta P/P$ increases from 10% to 30%. There is also a clear distinction among seasons, where winter-spring (DJF-MAM) tends to have larger values than summer-fall (JJA-SON). This can be explained by the higher evapotranspiration resulting from higher temperatures in the summer and fall seasons.

The trend in temperature sensitivity is similar to that of precipitation elasticity, except that the values are all negative (Fig. 10c, d). For the same amount of precipitation, higher temperature will lead to a larger evapotranspiration rate, which results in less runoff. The positive trend of the temperature sensitivity indicates that an additional unit increase of temperature will result in a smaller decrease of release. Regarding seasonality, temperature sensitivity behaves differently from precipitation elasticity. Compared to spring-summer (MAM-JJA), fall-winter (SON-DJF) has lower absolute $S_T(P, Q)$ and $S_T(P, S)$ values. This is because, in Texas, fall-winter (the cold season) is more water limited, which results in a smaller increase in ET than during spring-summer.

5. Conclusions

Due to the spatial heterogeneity and temporal variation of hydrological variables, it is impossible to provide constantly reliable and riskless water supply from unimpounded river flow. To increase the reliability and water-use flexibility, numerous reservoirs have been constructed around the world. Under the impacts of overwhelming environmental changes, how to best manage our water resources in a sustainable manner is a growing concern. However, robust estimation of future water availability is still facing great challenges because of the difficulties involved with link-

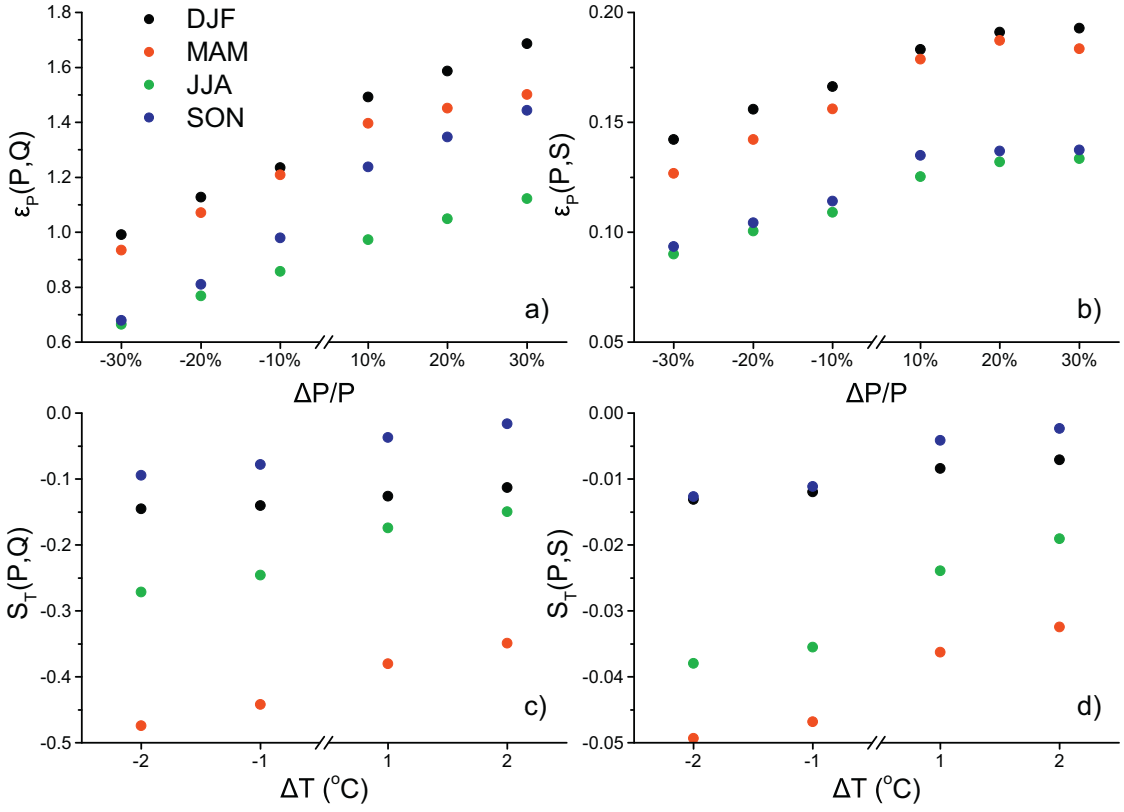

Fig. 10. Precipitation elasticity and temperature sensitivity for storage and release, with a) precipitation elasticity of release, b) precipitation elasticity of storage, c) temperature sensitivity of release, and d) temperature sensitivity of storage. (For interpretation of the references to colour in this figure legend, the reader is referred to the web version of this article.)

ing natural hydrological processes and reservoir operations. Therefore, in this study, a new reservoir module was incorporated into DHSVM to close this gap. The integrated modeling framework sets a base for improving the hyper-resolution representation of interdependent natural – human systems, and for supporting adaptation under non-stationary conditions. By conducting a case study using this integrated model, we have shown several outcomes:

- The model calibration and validation results (as shown in Figs. 6 and 7) suggest that the integrated model is able to capture the reservoir release and storage variations at a sub-monthly level. By adding reservoirs into DHSVM, the downstream flow values can be simulated more accurately.
- Reservoirs play an important role in streamflow regulation, especially with regard to flood control practices. After being rerouted by Lake Whitney, the upstream peak flows can almost always be controlled to under the downstream channel capacity.
- Our results have shown that both storage and release values are sensitive to several parameters—but especially to conservation pool storage. For Lake Whitney, conservation pool storage (which is a parameter that both storage and release values are sensitive to) has been changed several times in the 1960s to meet water management needs.
- Precipitation elasticity and temperature sensitivity of release and storage have been quantified. The precipitation elasticity of both release and storage increases when precipitation increases, but the scale varies by season. The temperature sensitivity of release and storage also shows a positive trend (in both cases), but the values are negative. These results can be beneficial for future flood and drought risk mitigation, which is important for a semi-arid climate watershed.

Even though the case study was carried out over USACE reservoirs, the integrated model is applicable for other reservoirs because most water management agencies use similar pool configurations. Model users can always tailor the settings to their own needs. For example, some reservoirs may not be used for flood control. This can be addressed by assigning a value of zero to the flood control pool volume in the module. If the reservoir has very limited information about the pool configuration, the corresponding parameter can also be obtained by calibration. This integrated model can also be coupled with optimization algorithms to improve the existing operation rules. Because the impoundment phase can be captured by the reservoir module, new reservoir design and operation rules can also be evaluated using our model. In addition, the capability of simulating hydropower generation can be beneficial for future energy management under the impact of global environmental changes.

While this module performs well in reservoir simulations, it does have some limitations. First of all, it is not a fully distributed reservoir module. Even though it can be located within a user-specified river segment, it cannot calculate the water interactions between the lake and its surrounding area in a distributed manner. To address this, we used an empirical monthly parameter (*MSRR*) to represent the process (Appendix A). In addition, this module was not designed to calculate daily hydropower water demand, which can be extremely complicated due to the highly variable electric energy consumption. Instead, it only uses a monthly value to represent the overall release for hydropower. Our primary objective was to integrate a reservoir module that can provide accurate sub-monthly storage and release values. Therefore, we expect that the integrated model can provide a platform that will contribute to water availability estimation at the watershed scale by including natural-human system interactions. Furthermore, it can be used to investigate the effects of climate change on water release (and

possible adaptation strategies, such as changes in operation rules, or by including a new reservoir) in terms of reservoir management practices.

Acknowledgement

This research was supported by U.S. National Science Foundation grant CBET-1454297. Gang Zhao was also partially supported by the W. G. Mills Scholarship (02-650509) and the USGS Graduate Student Research Program (G16AP00085) provided by the Texas Water Research Institute. We want to express our great appreciation to Michael F. Schwind (working for USACE) for sharing information about the reservoirs. This research has also benefitted from the use of the Texas A&M Supercomputing Facility (http://sc.tamu.edu) and the Oak Ridge Leadership Computing Facility (https://www.olcf.ornl.gov/). This paper was coauthored by employees of Oak Ridge National Laboratory, managed by UT Battelle, LLC, under contract DE-AC05-00OR22725, and the Pacific Northwest National Laboratory, managed by Battelle under contract DE-AC05-76RL01830 (both contracts are with the U.S. Department of Energy). Accordingly, the publisher, by accepting the article for publication, acknowledges that the United States government retains a nonexclusive, paid-up, irrevocable, worldwide license to publish or reproduce the published form of this manuscript, or allow others to do so, for United States government purposes.

Appendix

Table A1.

Table A1
Parameters defined and a detailed description of the reservoir module.

Parameter	Description	Symbol	Unit
Reservoir Name	Reservoir Name	/	/
Reservoir Index	The numbered index of the reservoir	/	/
Impoundment Date	Deliberate impoundment start date in MM/DD/YYYY	/	/
Initial Storage	Initial storage of reservoir if not simulated from deliberate impoundment	/	m^3
Inflow Segment	Inflow river segment (from DHSVM)	/	/
Volume of Capacity	Reservoir capacity volume	/	m^3
Volume of Flood Control Pool	Cumulative reservoir flood control pool volume	S_F	m^3
Volume of Conservation Pool	Cumulative reservoir conservation pool volume	S_C	m^3
Volume of Inactive Pool	Reservoir inactive pool volume	S_I	m^3
Discharge Coefficient[a]	Discharge coefficient from reservoir (empirical parameter associated with dam structure)	r	m^2/time step
Ratio of Flood Release Rate	Flooding condition multiplier (equals to 1 when inflow is not flood inflow, greater than 1 when inflow is flood inflow)	α	/
Flood Inflow Threshold[a]	Threshold to determine if inflow is flood inflow	Q_f^{in}	m^3/time step
Empirical Monthly Water Demand[a]	Downstream water demand (monthly values)	U_w [b]	m^3/time step
Monthly Water Withdraw	Direct water withdraw from reservoir (monthly values)	U_w [b]	m^3/time step
Ratio of Backflow	Backflow ratio of "Monthly Water Withdraw" (0–1)	r_b [c]	/
Monthly Soil Recharge Ratio[d]	Percentage of water relative to storage change that recharges surrounding soil (when elevation increases) or is discharged from surrounding soil to the reservoir (when elevation decreases) (0–1)	$MSRR$	/
Elevation-Volume Coefficients	Empirical coefficients in the Elevation-Volume relationship	α_H, β_H, γ_H	/
Surface Area-Volume Coefficients	Empirical parameters of Surface Area-Volume relationship	α_A, β_A, γ_A	/
Sedimentation Rate	Annual sedimentation rate	Δ_{sed}	m^3/time step
Sedimentation Start Year	Start year of sedimentation if not same as the model simulation start year (YYYY)	/	/
Number of Control Points	Number of downstream control points	/	/
Corresponding Segments	Segments in DHSVM for each "Control Point"	/	/
Streamflow Limits	Streamflow limits (channel capacity) for each "Control Point"	Q_{d_max}	m^3/time step
Close Time Weight[e]	Percentage of one time step to stop releasing water when downstream limit is passed (0–1)		/
Downstream Reservoir	Index number of immediate downstream reservoir		/
Hydropower[f]	If reservoir has hydropower facility		True/False
Power Stop Elevation	Elevation under which water level the hydropower will be stopped		m
Monthly Hydropower Water Demand[a]	Additional hydropower water release besides the "Downstream water demand" (monthly values)	U_w [b]	m^3/time step
Maximum Hydropower Turbine Capacity	Maximum hydropower turbine capacity	Q_{tur}	m^3/time step

[a] Calibrated parameters for the reservoirs.

[b] Because the regular monthly downstream water demand can be used to generate hydropower, the "Monthly Hydropower Water Demand" is additional water demand. "Monthly Water Withdraw" is the amount of water that was extracted from the reservoir directly without flowing through the dam structure.

[c] Back flow is for "Monthly Water Withdraw."

[d] To calculate the amount of water that exchanges with the surrounding soil, the Monthly Soil Recharge Ratio (MSRR) is calculated according to Equation A-1. Basically, if the water level increases at the current time step, part (i.e., MSRR) of the increased water will infiltrate the surrounding unsaturated soil. On the other hand, if the water level decreases at the current time step, the backflow will be recalculated using the storage difference, which is based on the mass balance.

$$Q_{soil} = \begin{cases} (S_n - S_{n-1}) * MSRR & (S_n > S_{n-1}) \\ (S_{n-1} - S_n) * \frac{MSRR}{1-MSRR} & (S_n < S_{n-1}) \end{cases} \quad (A-1)$$

[e] This parameter is designed for cases when the model running time step is too large to regulate the floodwater. In reality, when downstream control points are overloaded, the reservoir manager will close the gate until the downstream flooding situation is mitigated. However, when the model time step is too large (e.g., 1 day), the manager cannot close the gate for the entire time step. Thus, the gate closing time will be determined by the "model time step" multiplied by the "Close Time Weight." For example, the model time step is 3 days and the "Close Time Weight" is 1/3, so the gate will be closed for only 1 day if the downstream control points are flooding.

[f] Hydropower generation is calculated based on Equation A.2.

$$E_H = \begin{cases} \eta \cdot \gamma \cdot \gamma H \cdot Q \cdot \Delta t & 0 < Q \le Q_{tur} \\ \eta \cdot \gamma \cdot \gamma H \cdot Q_{tur} \cdot \Delta t & Q > Q_{tur} \end{cases} \quad (A-2)$$

where E_H is the generated hydroelectric energy (Watt * hour); η is the generation efficiency (0.85 for this study); γ is the specific weight of water (9800 N/m^3); ΔH is the effective head (m) approximated as the elevation difference between reservoir water surface elevation and turbine elevation; Q is the flow magnitude (m^3/s); and Δt is the hydropower modeling time step (hours). If Q is greater than the turbine capacity Q_{tur}, then only Q_{tur} is used for hydropower generation (and the rest is spilled directly).

References

Adam, J., Stephens, J., Chung, S., Brady, M., Evans, R.D., Kruger, C., et al., 2014. BioEarth: envisioning and developing a new regional earth system model to inform natural and agricultural resource management. Clim. Change 129, 555–571. http://dx.doi.org/10.1007/s10584-014-1115-2.

Arnold, J.G., Fohrer, N., 2005. SWAT2000: current capabilities and research opportunities in applied watershed modelling. Hydrol. Processes 19, 563–572. http://dx.doi.org/10.1002/hyp.5611.

Bader D., W. Collins, R. Jacob, P. Jones, P. Rasch, M. Taylor, et al. Accelerated climate modeling for energy (ACME) project strategy and initial implementation plan. Available online at http://climatemodeling.science.energy.gov/. (2014).

Battin, J., Wiley, M.W., Ruckelshaus, M.H., Palmer, R.N., Korb, E., Bartz, K.K., et al., 2007. Projected impacts of climate change on salmon habitat restoration. Proc. Natl. Acad. Sci. 104, 6720–6725. http://dx.doi.org/10.1073/pnas.0701685104.

Biemans, H., Haddeland, I., Kabat, P., Ludwig, F., Hutjes, R.W.A., Heinke, J., et al., 2011. Impact of reservoirs on river discharge and irrigation water supply during the 20th century. Water Resour. Res. 47. http://dx.doi.org/10.1029/2009WR008929.

Brune, G.M., 1953. Trap efficiency of reservoirs. Eos. Trans. Am. Geophys. Union 34, 407–418.

Chao, B.F., Wu, Y., Li, Y., 2008. Impact of artificial reservoir water impoundment on global sea level. Science 320, 212–214.

Christensen, N., Wood, A., Voisin, N., Lettenmaier, D., Palmer, R., 2004. The effects of climate change on the hydrology and water resources of the Colorado River Basin. Clim. Change 62, 337–363. http://dx.doi.org/10.1023/B:CLIM.0000013684.13621.1f.

Conway, D., 1996. The impacts of climate variability and future climate change in the Nile Basin on water resources in Egypt. Int. J. Water Resour. Develop. 12, 277–296.

Croley, T.E., He, C., 2005. Distributed-parameter large basin runoff model. I: model development. J. Hydrol. Eng. 10, 173–181.

Cuo, L., Lettenmaier, D.P., Mattheussen, B.V., Storck, P., Wiley, M., 2008. Hydrologic prediction for urban watersheds with the distributed hydrology–soil–vegetation model. Hydrol. Processes 22, 4205–4213.

Cuo, L., Lettenmaier, D.P., Alberti, M., Richey, J.E., 2009. Effects of a century of land cover and climate change on the hydrology of the Puget Sound basin. Hydrol. Processes 23, 907–933. http://dx.doi.org/10.1002/hyp.7228.

Doten, C.O., Bowling, L.C., Lanini, J.S., Maurer, E.P., Lettenmaier, D.P., 2006. A spatially distributed model for the dynamic prediction of sediment erosion and transport in mountainous forested watersheds. Water Resour. Res. 42.

Fekete, B.M., Wisser, D., Kroeze, C., Mayorga, E., Bouwman, L., Wollheim, W.M., et al., 2010. Millennium ecosystem assessment scenario drivers (1970–2050): climate and hydrological alterations. Global Biogeochem. Cycles 24.

Gallego-Elvira, B., Baille, A., Martín-Górriz, B., Martínez-Álvarez, V., 2010. Energy balance and evaporation loss of an agricultural reservoir in a semi-arid climate (south-eastern Spain). Hydrol. Processes 24, 758–766.

Gökbulak, F., Özhan, S., 2006. Water Loss Through Evaporation from Water Surfaces of Lakes and Reservoirs in Turkey. Official Publication of the European Water Association, EWA.

Graf, W.L., 1999. Dam nation: a geographic census of American dams and their large-scale hydrologic impacts. Water Resour. Res. 35, 1305–1311. http://dx.doi.org/10.1029/1999WR900016.

Graf, W.L., 2006. Downstream hydrologic and geomorphic effects of large dams on American rivers. Geomorphology 79, 336–360.

Gutierrez, F., Dracup, J., 2001. An analysis of the feasibility of long-range streamflow forecasting for Colombia using El Nino–Southern Oscillation indicators. J. Hydrol. 246, 181–196.

Haddeland, I., Lettenmaier, D.P., Skaugen, T., 2006. Effects of irrigation on the water and energy balances of the Colorado and Mekong river basins. J. Hydrol. 324, 210–223. http://dx.doi.org/10.1016/j.jhydrol.2005.09.028.

Hamlet, A.F., Lettenmaier, D.P., 1999. Effects of climate change on hydrology and water resources in the Columbia River Basin. JAWRA J. Am. Water Resour. Assoc. 35, 1597–1623. http://dx.doi.org/10.1111/j.1752-1688.1999.tb04240.x.

Hanasaki, N., Kanae, S., Oki, T., 2006. A reservoir operation scheme for global river routing models. J. Hydrol. 327, 22–41.

Homer, C., Dewitz, J., Fry, J., Coan, M., Hossain, N., Larson, C., et al., 2007. Completion of the 2001 National Land Cover Database for the Counterminous United States. Photogramm. Eng. Remote Sens. 73, 337.

HydroLogics Inc, 2007. User manual for OASIS with OCL, Columbia, MD.

Jarvis, A., Reuter, H.I., Nelson, A., Guevara, E., 2008. Hole-Filled Srtm for the Globe Version 4 Available from the CGIAR-CSI SRTM 90 m Database (http://srtm.csi.cgiar.org).

Kavvas, M., Chen, Z.-Q., Tan, L., Soong, S.-T., Terakawa, A., Yoshitani, J., et al., 1998. A regional-scale land surface parameterization based on areally-averaged hydrological conservation equations. Hydrol. Sci. J. 43, 611–631.

Kraucunas, I., Clarke, L., Dirks, J., Hathaway, J., Hejazi, M., Hibbard, K., et al., 2015. Investigating the nexus of climate, energy, water, and land at decision-relevant scales: the platform for regional integrated modeling and analysis (PRIMA). Clim. Change 129, 573–588. http://dx.doi.org/10.1007/s10584-014-1064-9.

Labadie, J., Larson, R., 2007. MODSIM 8.1: River Basin Management Decision Support System. Colorado State University, Fort Collins, p. 123. User Manual and Documentation.

Lehner, B., Liermann, C.R., Revenga, C., Vörösmarty, C., Fekete, B., Crouzet, P., et al., 2011. High-resolution mapping of the world's reservoirs and dams for sustainable river-flow management. Front. Ecol. Env. 9, 494–502.

Liu, X., Tang, Q., Voisin, N., Cui, H., 2016. Projected impacts of climate change on hydropower potential in China. Hydrol. Earth Syst. Sci. Discuss. 2016, 1–30.

Livneh, B., Rosenberg, E.A., Lin, C., Nijssen, B., Mishra, V., Andreadis, K.M., et al., 2013. A long-term hydrologically based dataset of land surface fluxes and states for the conterminous United States: update and extensions. J. Clim. 26, 9384–9392.

Livneh, B., Bohn, T.J., Pierce, D.W., Munoz-Arriola, F., Nijssen, B., Vose, R., et al., 2015. A spatially comprehensive, hydrometeorological data set for Mexico, the U.S., and Southern Canada 1950–2013. Sci. Data 2, 150042. http://dx.doi.org/10.1038/sdata.2015.42.

Lund, J.R., Ferreira, I., 1996. Operating rule optimization for Missouri River reservoir system. J. Water Resour. Plann. Manag.-Asce 122, 287–295. http://dx.doi.org/10.1061/(asce)0733-9496(1996)122:4(287).

Mahmood, K., 1987. Reservoir Sedimentation: Impact, Extent, and Mitigation. International Bank for Reconstruction and Development, Washington, DC (USA) Technical paper.

Mateo, C.M., Hanasaki, N., Komori, D., Tanaka, K., Kiguchi, M., Champathong, A., et al., 2014. Assessing the impacts of reservoir operation to floodplain inundation by combining hydrological, reservoir management, and hydrodynamic models. Water Resour. Res. 50, 7245–7266. http://dx.doi.org/10.1002/2013WR014845.

Milly, P.C.D., Betancourt, J., Falkenmark, M., Hirsch, R.M., Kundzewicz, Z.W., Lettenmaier, D.P., et al., 2008. Stationarity is dead: whither water management? Science 319, 573–574. http://dx.doi.org/10.1126/science.1151915.

Moy, W.-S., Cohon, J.L., ReVelle, C.S., 1986. A programming model for analysis of the reliability, resilience, and vulnerability of a water supply reservoir. Water Resour. Res. 22, 489–498. http://dx.doi.org/10.1029/WR022i004p00489.

Nash, L.L., Gleick, P.H., 1991. Sensitivity of streamflow in the Colorado Basin to climatic changes. J. Hydrol. 125, 221–241. http://dx.doi.org/10.1016/0022-1694(91)90030-L.

Naz, B.S., Frans, C.D., Clarke, G.K.C., Burns, P., Lettenmaier, D.P., 2014. Modeling the effect of glacier recession on streamflow response using a coupled glacio-hydrological model. Hydrol. Earth Syst. Sci. 18, 787–802. http://dx.doi.org/10.5194/hess-18-787-2014.

Oki, T., Kanae, S., 2006. Global hydrological cycles and world water resources. Science 313, 1068–1072.

Penman, H.L., 1948. Natural evaporation from open water, bare soil and grass. In: Proceedings of the Royal Society of London A: Mathematical, Physical and Engineering Sciences. The Royal Society, pp. 120–145.

Sankarasubramanian, A., Vogel, R.M., Limbrunner, J.F., 2001. Climate elasticity of streamflow in the United States. Water Resour. Res. 37, 1771–1781.

Schaake, J.C., 1990. From Climate to Flow. John Wiley and Sons Inc., New York, pp. 177–206.

Seager, R., Harnik, N., Robinson, W.A., Kushnir, Y., Ting, M., Huang, H.P., et al., 2005. Mechanisms of ENSO-forcing of hemispherically symmetric precipitation variability. Quart. J. R. Meteorol. Soc. 131, 1501–1527. http://dx.doi.org/10.1256/qj.04.96.

Shiklomanov, I.A., 2000. Appraisal and assessment of world water resources. Water Int. 25, 11–32.

Soil Survey Staff, 2016. Natural Resources Conservation Service, United States Department of Agriculture. Web Soil Survey Available online at http://websoilsurvey.nrcs.usda.gov/.

Stocker, T., Qin, D., Plattner, G., Tignor, M., Allen, S., Boschung, J., et al., 2013. Climate change 2013: the physical science basis. Contribution of working group I to the fifth assessment report of the intergovernmental panel on climate change.

Sun, N., Yearsley, J., Voisin, N., Lettenmaier, D.P., 2015. A spatially distributed model for the assessment of land use impacts on stream temperature in small urban watersheds. Hydrol. Processes 29, 2331–2345. http://dx.doi.org/10.1002/hyp.10363.

Texas Water Development Board, 2006. Volumetric Survey of Lake Whitney Available online at http://www.twdb.texas.gov/hydro_survey/whitney/2005-06/Whitney2005_FinalReport.pdf.

Texas Water Development Board, 2009. Volumetric Survey of Aquilla Lake Available online at http://www.twdb.texas.gov/hydro_survey/aquilla/2008-03/AquillaLake2008_FinalReport.pdf.

U.S. Bureau of Reclamation, 1991. HYDROSS version 4.3 user's manual, Information Resources Division. Bureau of Reclamation, Billings, MT.

VanRheenen, N., Wood, A., Palmer, R., Lettenmaier, D., 2004. Potential implications of PCM climate change scenarios for Sacramento–San Joaquin River Basin hydrology and water resources. Clim. Change 62, 257–281. http://dx.doi.org/10.1023/B:CLIM.0000013686.97342.55.

Voisin, N., Li, H., Ward, D., Huang, M., Wigmosta, M., Leung, L., 2013. On an improved sub-regional water resources management representation for integration into earth system models. Hydrol. Earth Syst. Sci. 17, 3605–3622.

Voisin, N., Liu, L., Hejazi, M., Tesfa, T., Li, H., Huang, M., et al., 2013. One-way coupling of an integrated assessment model and a water resources model: evaluation and implications of future changes over the US Midwest. Hydrol. Earth Syst. Sci. 17, 4555–4575. http://dx.doi.org/10.5194/hess-17-4555-2013.

Voisin, N., Hejazi, M., Leung, L.R., Liu, L., Huang, M., Li, H., et al., 2015. Representing Groundwater Use and Return Flow and their Signatures on Surface Hydrology and Water Stress in Integrated Water Models. Pacific Northwest National Laboratory, Richland, WA PNNL-SA-109215[submitted].

Vörösmarty, C.J., Green, P., Salisbury, J., Lammers, R.B., 2000. Global water resources: vulnerability from climate change and population growth. Science 289, 284–288. http://dx.doi.org/10.1126/science.289.5477.284.

Wigmosta, M.S., Vail, L.W., Lettenmaier, D.P., 1994. A distributed hydrology-vegetation model for complex terrain. Water Resour. Res. 30, 1665–1679. http://dx.doi.org/10.1029/94WR00436.

Wood, E.F., Roundy, J.K., Troy, T.J., van Beek, L.P.H., Bierkens, M.F.P., Blyth, E., et al., 2011. Hyperresolution global land surface modeling: meeting a grand challenge for monitoring Earth's terrestrial water. Water Resour. Res. 47. http://dx.doi.org/10.1029/2010WR010090.

World Commission on Dams, 2000. Dams and Development: A New Framework for Decision Making. Earthscan, London, UK.

Wurbs, R.A., 1996. Modeling and Analysis of Reservoir System Operations. Prentice Hall.

Wurbs, R., 2012. Water Rights Analysis Package (WRAP) Modeling System Reference Manual. Texas Water Resources Institute.

Yates, D., Sieber, J., Purkey, D., Huber-Lee, A., 2005. WEAP21—A demand-, priority-, and preference-driven water planning model: part 1: model characteristics. Water Inte. 30, 487–500.

Zagona, E.A., Fulp, T.J., Shane, R., Magee, T., Goranflo, H.M., 2001. Riverware: A generalized tool for complex reservoir system modeling. JAWRA J. Am. Water Resour. Assoc. 37, 913–929. http://dx.doi.org/10.1111/j.1752-1688.2001.tb05522.x.

Zhao, G., Gao, H., Cuo, L., 2016. Effects of urbanization and climate change on peak flows over the San Antonio River Basin, Texas. J. Hydrometeorol 17, 2371–2389. http://dx.doi.org/10.1175/JHM-D-15-0216.1.

Zhou, T., Nijssen, B., Gao, H., Lettenmaier, D.P., 2016. The contribution of reservoirs to global land surface water storage variations. J. Hydrometeorol. http://dx.doi.org/10.1175/JHM-D-15-0002.1.